

CRYOGENICS AND LHC BEAM COMMISSIONING

L. Tavian, CERN, Geneva, Switzerland

Abstract

During the LHC beam commissioning, the cryogenic system must fulfil its requirements and give maximum availability to the beam. The cooling principle of the magnet at 1.9 K will be recalled in this paper with particular emphasis on the response of the cryogenic system during the cycle of injection, ramp, store and de-ramp. The cryogenic conditions to allow magnet powering will be listed. The different limitations due to the cryogenic system in terms of cycle frequency, magnet temperature profile stability, as well as quench recovery speed will be also described.

1 INTRODUCTION

The superconducting magnets of the LHC are cooled at 1.9 K with superfluid helium [1]. Cryogenic plants located at the 8 access points cool separate sectors with slopes up to 1.4 %. Beam screens, heat intercepts and thermal shields have been implemented and optimised to reduced heat loads entering the magnet cold-masses. Nevertheless, this temperature level has to cope with static heat inleaks, steady-state dynamic heat loads such as resistive dissipation in splices and beam gas scattering, as well as transient heat dissipations such as eddy-current losses during magnet ramping and heating during resistive transition of magnets. During the LHC beam commissioning, the cryogenic system must give a optimum availability to the beam.

2 COOLING PRINCIPLE OF MAGNETS

2.1 Basic cryogenic sectorisation

In order to reduce the hydrostatic head in the magnet cooling circuits due to the tunnel slope as well as to limit the hydraulic propagation of resistive transitions, plugs sub-divide each sector in smaller magnet strings. Figure 1 shows the basic cryogenic sectorisation of the 1.9 K superfluid circuits [2,3]. One arc, which contains 27 cells, is divided in 13 sub-sectors, each constituted of 2 or 3 cells.

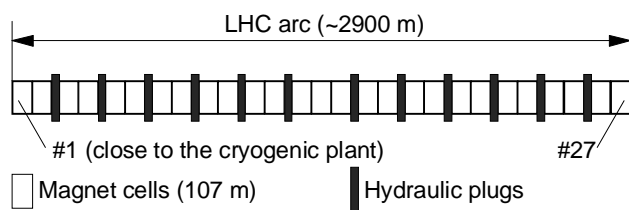


Figure 1: Basic cryogenic sectorisation

2.2 Cell cooling principle

Within a cell, the magnets are cooled in pressurised superfluid helium baths [4] by a distributed bayonet heat exchanger [5] in which saturated superfluid helium flows [6]. Figure 2 shows the cooling principle of magnet cells. The bayonet heat exchanger is supplied with supercritical helium (SHe) at 2.2 K, which is expanded in a Joule-Thomson valve (JT). The pressure in the heat exchanger is maintained by a pumping system common to a sector. Each magnet is equipped with a temperature sensor. The JT valve controls a temperature difference of 30 mK between the highest temperature of cell magnets and the saturated temperature T_{s0} corresponding to the pressure P_{s0} at the heat exchanger outlet. This control method [7] has been validated on the String 1 experiment. Thanks to the huge heat conductivity of superfluid helium, this control method allows to reduce considerably the time response of the corresponding loop. The bayonet heat exchanger has a linear conductance of 122 W/m.K, i.e. with a complete wetted heat exchanger and with a temperature difference of 30 mK, a power of 390 W per cell can be extracted. As a consequence, the bayonet heat exchanger is partially dry to match smaller power dissipation per cell.

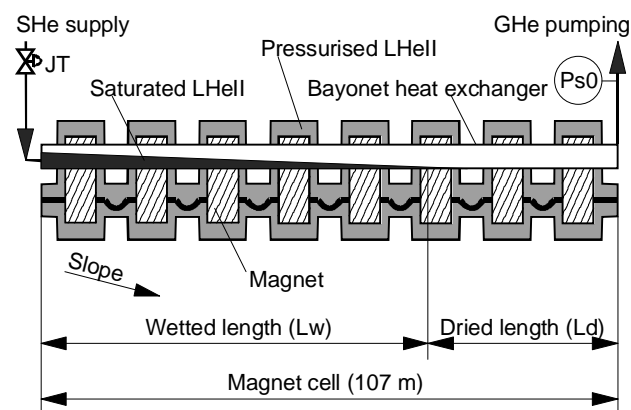


Figure 2: Cell cooling principle

3 COLD-MASS HEAT LOADS

3.1 Steady state heat loads

Five different operation modes have been identified for beam operation:

- The injection standby operation with a beam energy of 450 GeV.

- The low beam intensity operation with a beam energy of 7 TeV but with reduced beam current.
- The nominal operation with a beam energy of 7 TeV and a beam current of 0.56 A.
- The ultimate operation with a beam energy of 7 TeV but with a beam current of 0.85 A.
- The installed operation which corresponds to the nominal operation with uncertainty and over-capacity coefficients.

Table 1 gives the heat loads entering the cold masses per cell for the different operation modes. During the beam commissioning, only the two first operation modes have to be considered. Concerning beam gas scattering losses, between nominal and ultimate operation, the assumption is made that the improvement of the beam vacuum compensates the increase of the beam current. Consequently, the total heat load stays at the same level.

Table 1: Steady state heat loads per cell

Heat load [W]	Injection Standby	Low- beam intensity	Nominal & Ultimate	Installed
Static heat inleak	28.8	28.8	28.8	54.0
Resistive heating	~ 0	11.4	11.4	17.1
Beam-gas scattering	~ 0	~ 0	6.2	9.3
Total	28.8	40.2	46.4	80.4

3.2 Transient heat loads

During LHC operation, the transient operations are listed hereafter:

- The magnet current ramp-up from 0 to 12 kA with a rate of 10 A/s, for which Eddy currents dissipate 400 J/m in the cold masses.
- The magnet current de-ramp from 12 to 0 kA with a rate of 10 A/s, for which Eddy currents dissipate 400 J/m in the cold masses.
- The magnet current fast ramp-down from 12 to 0 kA with a rate of 100 A/s, for which Eddy currents dissipate 2800 J/m in the cold masses.
- The local random losses which can dissipate in the cold masses extra heat loads up to 33 W per cell.
- The beam squeezing which can dissipate in few tens of seconds an additional power up to 420 W per inner triplet close to the large LHC experiments.
- The limited resistive transition of magnets which warms the corresponding string up to 30 K.

The three first transient operations are buffered by the helium contained in the cold masses with an average contents of 15 l/m. The full sector resistive transition is considered as an accidental event and is not treated hereafter.

4 TEMPERATURE STABILITY IN STEADY STATE OPERATION

4.1 Stability of the control loop

In steady state operation, for a given heat load, the control loop and the corresponding JT valve opening variation gives magnet temperature variation of about ± 5 mK. This stability has been measured and validated on the String 1 experiment [8].

4.2 Stability in between operation modes

In the cell, the wetted length increases with the heat load deposition. In a sub-sector, the dried lengths are cooled by conduction in superfluid helium, which has a free cross-section of 60 cm². The corresponding power is thus extracted by the wetted part. Depending on their location with respect to the hydraulic plugs, the dried length can be cooled by one or two wetted lengths. As a consequence, the highest magnet temperature inside a cell does not always correspond to the magnet located at the end of the dried length. In addition, the location of the highest magnet temperature can move with respect to the heat load. Figure 3 and 4 show the temperature difference evolution with respect to the temperature Ts0 for the different operation modes. The horizontal parts correspond to the wetted areas. This temperature difference can increase or decrease depending on the magnet location. The maximum temperature difference for one given magnet is 15 mK for a 2-cell sub-sector and 12 mK for a 3-cell sub-sector.

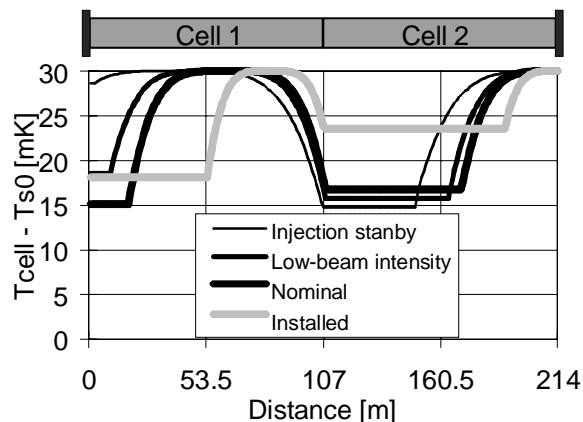


Figure 3: Temperature difference evolution for 2-cell sub-sectors

To obtain the magnet temperature profile, the temperature Ts0 has to be estimated taking into account the pressure drop in the pumping line, which increases with the sector heat load to be extracted, as well as the hydrostatic head due to the tunnel slope. Figure 5 shows the temperature evolution for the LHC sector 4-5, which corresponds to a high-loaded sector coupled with the highest elevation difference. This combination gives the

highest temperature excursions. For this sector, the arc magnet temperature stays below 1.9 K. The maximum temperature difference between “Injection Standby” and “Ultimate” operation is 68 mK. During LHC beam commissioning, with heat loads corresponding to “Low beam intensity” operation, the temperature difference will be limited to 24 mK.

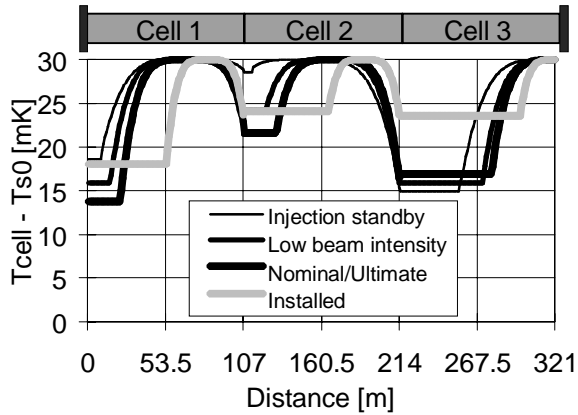


Figure 4: Temperature difference evolution for 3-cell sub-sectors

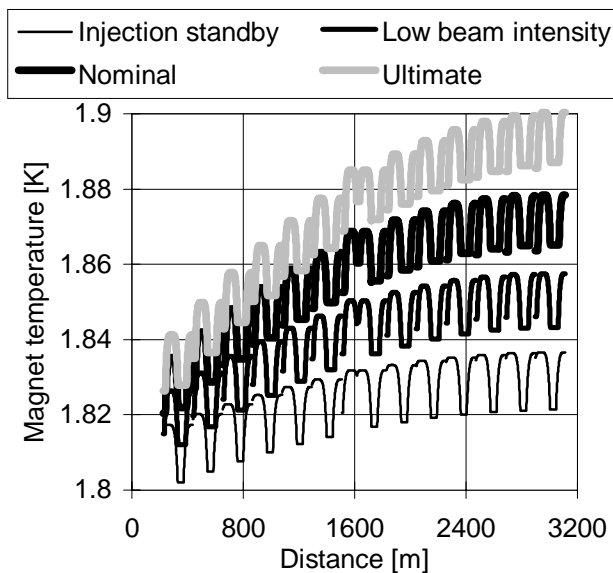


Figure 5: Temperature evolution of the sector 4-5

5 TEMPERATURE STABILITY IN TRANSIENT OPERATIONS

5.1 Current ramp and de-ramp

The cryogenic system allows the magnet when the following conditions are fulfilled:

- the magnet temperatures are correct,
- the helium levels and current lead temperatures of distribution feed boxes are correct,
- the cryogenic plant process is correct,

- the quench buffers and the cold recovery line are empty.

When this authorisation is sent, each sub-system is self protected and any red light requiring a magnet de-ramp will be emitted by the cryogenic system.

During LHC beam commissioning it is foreseen to make a pre-cycle of the magnets before the injection phase. The corresponding current rate of 10 A/s produces a heat dissipation of 400 J/m per ramp. Another source of dissipation concerns the resistive heating in superconductor splices. This energy is buffered by the helium content of 15 l/m, which limits the cold mass temperature excursion. During this phase, the cryogenic system participates actively at the magnet temperature recovery by increasing the pumping capacity. Figure 6 shows the temperature excursion of the magnet cold-masses during this ramping process as well as the evolution of the pumping capacity. Depending of the cell location, the temperature excursions of the cold-masses vary from 20 up to 50 mK. The active cooling is more efficient for the cells close to the cryogenic plant where the pumping line pressure drops are reduced. These temperature excursions are small enough to keep the magnet temperature below 1.9 K.

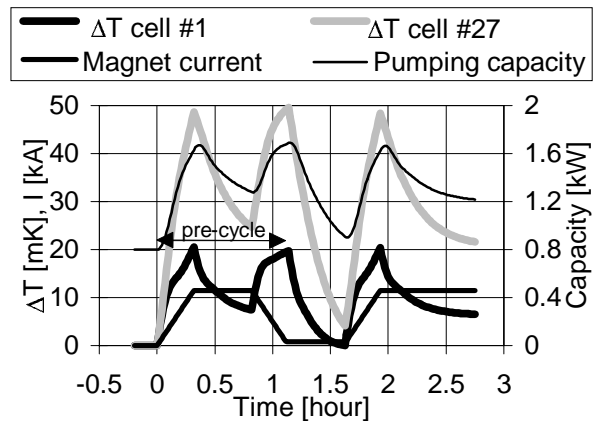


Figure 6: Temperature excursion during an injection sequence

The normal rate of injection is twice a day. During the beam commissioning, the injection rate will probably be higher. Figure 7 shows the temperature excursion during continuous sequences of current ramp and de-ramp. Depending on the cell location, the temperature excursions vary from 30 to 70 mK, i.e. the maximum magnet temperature of 1.9 K. In fact, these ramp sequences, which correspond to an average pumping capacity of 1.94 kW, are in accordance with the installed pumping capacity of 2.4 kW per sector. The cryogenic system will not limit the frequency of injection sequences during the beam commissioning.

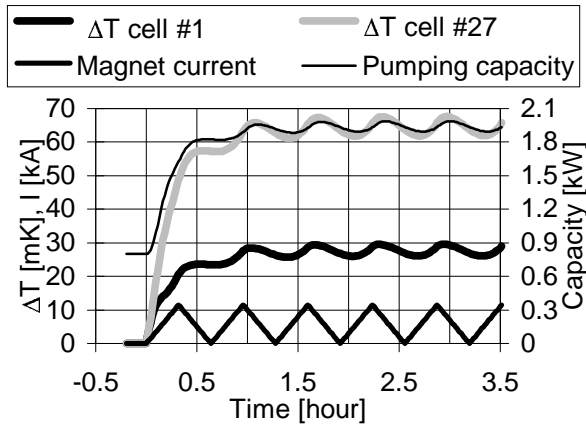


Figure 7: Temperature excursion during continuous sequences of current ramp and de-ramp

5.2 Fast current ramp-down

In case of problems with the powering system and/or magnets, fast current ramp-down can be performed with a current rate variation of 100 A/s, which dissipates 2800 J/m in the magnet cold-masses. Figure 8 shows the temperature excursions and the pumping capacity evolution during a fast current ramp-down. The temperature excursion is about 250 mK, i.e., magnet temperatures increase close to the $T\lambda$ temperature. Using the full pumping capacity, the re-cool-down time after a fast current ramp-down is about 2 hours.

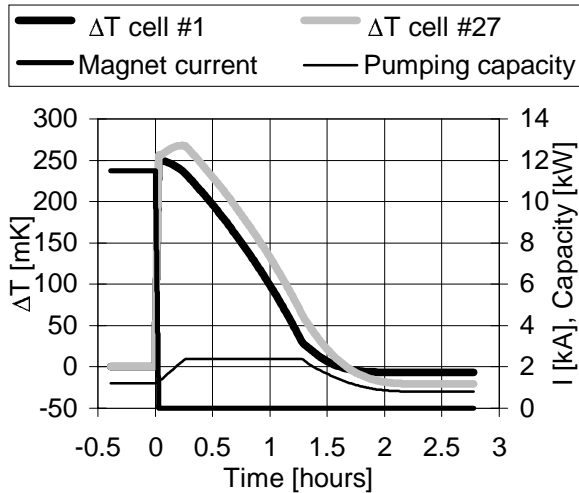


Figure 8: Temperature excursions during fast current ramp-down

5.3 Local random loss dissipation

The beam cleaning inefficiency can produce local random loss dissipation of about 33 W in cells of dispersion suppressors. The location of this heat load depends on the correction scheme and can change very rapidly. The control loop has to cope with a very fast transient mode. Figure 9 shows the temperature profile

of a 2-cell sub-sector in nominal operation with and without local random loss dissipation entering the first cell.

Table 2 gives the main characteristics of a control loop. The total time to reach the temperature profile with local random losses is about 8 minutes. During this time the loop is not in equilibrium; consequently the magnet temperature increases with a maximum temperature excursion of 20 mK. This temperature excursion is acceptable and does not require feed-forward control. This assessment assumes that during the response time no extra heat load is extracted. This assumption maximises the temperature excursion.

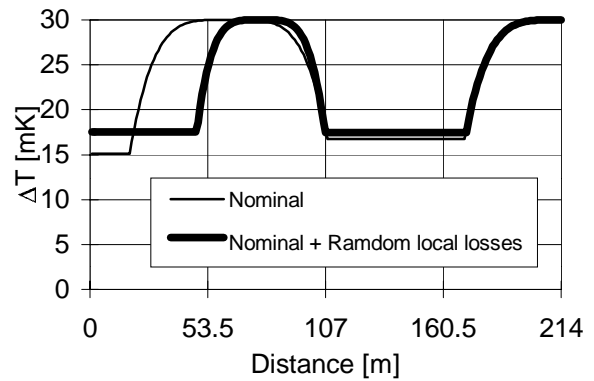


Figure 9: Temperature profile in nominal operation with and w/o local random losses

Table 2: Characteristics of local random loss control

Characteristics	Unit	Value
Wetted length without random losses	[m]	18.5
Wetted length with random losses	[m]	30
Liquid helium velocity	[m/s]	0.1
Time response of the control loop	[s]	185
Time for liquid helium progression	[s]	300
Total time response	[s]	485
Local random losses	[W]	33
Extra energy deposition	[kJ]	16
Mass of helium per cell	[kg]	237
Internal energy increase	[J/kg]	67.5
Temperature excursion	[mK]	20

5.4 Beam squeezing

The heat induced by the beam squeezing is proportional to the luminosity and is deposited in the cold-masses of the Inner Triplets of the sectors by a very fast process. Due to the huge ratio between this dynamic heat load and the static heat inleaks, which is about 10 for the nominal luminosity and 25 for the ultimate luminosity, the dynamic adaptation of the corresponding loops must be produced by feed-forward control. Nevertheless, during the LHC beam commissioning, the corresponding low luminosity will give ratios below 3, which does not require any special feed-forward control.

5.5 Limited resistive transition

A limited resistive transition [9] concerns up to 4 cells. This resistive transition is not considered as an accidental event and can appear frequently. As a comparison, the HERA collider at DESY has to cope with such an event once per week.

After a limited resistive transition, the corresponding cells have to be re-cooled from 30 down to 4.5 K and filled up to 70 % by the main 4.5 K refrigerator [10]. Then, filling up to 100 % as well as cool-down from 4.5 to 1.9 K have to be performed using the 1.8 K refrigeration unit [11] coupled to the 4.5 K refrigerator. Table 3 gives the recovery capacities for limited resistive transitions of 1 and 4 cells. During the recovery, in addition to the cool-down of the quenched magnets, the cryogenic system has to re-cool the other cells, which have withstood a fast current ramp-down, and keep them in normal operation. As a consequence, the re-cool-down capacity is limited to the remaining over-capacity. Other limitations come from the maximum flow-rate related to a single loop.

Figure 10 shows the operation times required for the different phases. The recovery time is 6.8 hours for a four-cell resistive transition and 3.7 hours for a single-cell resistive transition. The minimum possible recovery time corresponds to a fast current ramp-down and takes 2 hours.

Table 3: Characteristics of limited resistive transitions

Characteristics		1 cell	4 cells
Max. cool-down and filling flow per cell	[g/s]	100	37.5
Average filling rate from 70 to 100 % per cell	[g/s]	62	20
Cool-down capacity from 4.5 to 1.9 K per cell	[W]	480	375

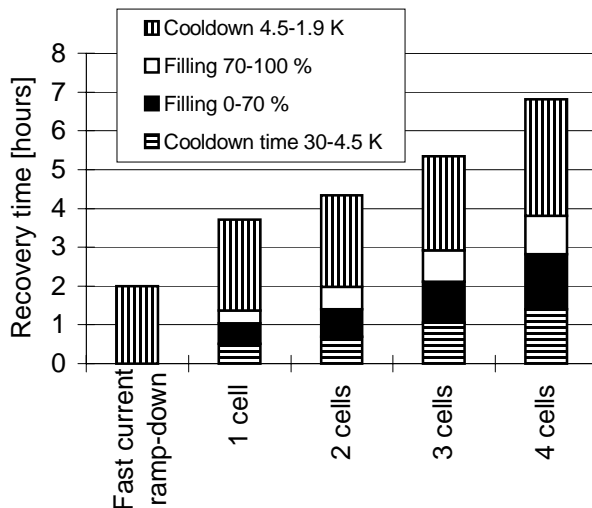


Figure 10: Recovery time after a limited resistive transition

6 CONCLUSION

In steady state operation, the cooling principle of the magnets maintains the arc magnet temperature below 1.9 K and keeps the temperature stability within 5 mK. In between the different steady state operation modes, the temperature stability is within 70 mK; during the beam commissioning, at low-beam intensity, only 25 mK is expected.

Concerning transient operation modes, the maximum temperature excursion during injection sequence is 50 mK. The cryogenic system will not limit the frequency of injection cycles. During fast current ramp-down the magnet temperatures stay below $T\lambda$, but a recovery time of 2 hours is required. Local random losses give temperature excursion of 20 mK. The heat load level during beam commissioning due to beam squeezing will be low enough to avoid control based on feed-forward. Depending on the number of magnets involved, limited resistive transition will produce beam downtime of 2 to 7 hours.

During the different steady-state and transient operation modes, the temperature stability and excursions are limited and give acceptable changes in persistent current.

REFERENCES

- [1] Ph. Lebrun, "Cryogenic for the Large Hadron Collider", invited paper presented at MT16, Ponte Vedra Beach, USA (1999)
- [2] M. Chorowski *et al.*, "A simplified cryogenic distribution scheme for the LHC", *Adv. Cryo. Eng.* **43A** (1998) 395-402.
- [3] M. Chorowski *et al.*, "A proposal for simplification of the LHC cryogenic scheme", LHC Project Note 106.
- [4] Ph. Lebrun, "Superfluid helium as a technical coolant", Atti XV Congresso Nazionale sulla Trasmissione del Calore, Edizioni ETS, Politecnico di Torino, Italy (1997) 61-77
- [5] Ph. Lebrun *et al.*, "Cooling string of superconducting devices below 2 K: the helium II bayonet heat exchanger", *Adv. Cryo. Eng.* **43A** (1998) 419-426
- [6] A. Gauthier *et al.*, "Thermodynamic behaviour of HeII in stratified co-current two-phase flow", Proc. ICEC16, Elsevier Science, Oxford, UK (1997) 519-522.
- [7] E. Blanco-Vinuela *et al.*, "Linear model-based predictive control of the LHC 1.8 K cryogenic loop", paper presented at CEC99, Montréal (1999)
- [8] J. Casas-Cubillos *et al.*, "Operation, testing and long-term behaviour of the LHC Test String cryogenic system", Proc. ICEC17, IoP, Bristol, UK (1998), 747-750.
- [9] M. Chorowski *et al.*, "Thermohydraulics of quenches and helium recovery in the prototype magnet strings", *Cryogenics* **38** (1998) 533-543.
- [10] S. Claudet *et al.*, "Specification of four new large 4.5 K helium refrigerators for the LHC", paper presented at CEC99, Montréal (1999)
- [11] S. Claudet *et al.*, "Specification of eight 2400 W @ 1.8 K refrigeration units for the LHC", paper presented at ICEC18, Mumbai India (2000)